which started with D_{4h} symmetry (equalized C–C bond lengths of 140.9 pm) and optimized the geometry while preserving the planarity. For the tetraoxaporphyrin dication and dianion, the optimized structures had still D_{4h} symmetry with C–C bond lengths of 140 ± 3 pm, whereas for the tetraoxaisophlorin the symmetry was lowered to D_{2h} with these bond lengths alternating between 136 ± 2 and 145 ± 2 pm (AM1) or 138 ± 2 and 147 ± 2 pm (MNDO).

At present, experimental evidence for double-bond localization solely rests upon the observation of the weak long-wave absorption assigned to the $b_{3g} \leftarrow b_{2g}$ transition. X-ray crystallographic structure analysis of tetraoxaisophlorin[4] shows an averaged geometry, caused by superposition of reflexes arising from molecules differently oriented in the unit cells. Neither is reduction of symmetry from D_{4h} to D_{2h}, as a consequence of double-bond localization, indicated by ^{1}H and ^{13}C NMR spectra above 138 K.[4] Hereto, one may consider the corresponding results for the recently synthesized 2,3,7,8,12,13,17,18-octaethyl-*N*,*N*′,*N*″,-*N*‴-tetramethylisophlorin[20] which is iso-π-electronic with tetraoxaisophlorin but, in contrast to this molecule, has a nonplanar geometry. The ^{1}H NMR spectra of the octaethyl-*N*,*N*′,*N*″,-*N*‴-tetramethylisophlorin, taken in the range 201–377 K, exhibit a dynamic process diagnostic of an interconversion between two degenerate structures with localized double bonds. The coalescence temperature and the free energy of bond-shift activation are T_c = 289 K and $\Delta G^{\ddagger}$ = 55.2 kJ/mol (13.2 kcal/mol).[20] A $\Delta G^{\ddagger}$ value of 55.7 kJ/mol (13.3 kcal/mol), which is equal within the limits of experimental error, results from the formula[21]

$$\Delta G^{\ddagger} = 19.13T_c\left(9.97 + \log\frac{T_c}{\delta\nu}\right) \text{ [J/mol]}$$

where $\delta\nu$ = 230 Hz is the difference in the positions of coalescing NMR signals of the NCH_3 protons. Application of this formula to tetraoxaisophlorin with $\delta\nu$ = 120 Hz[22] and T_c < 138 K yields $\Delta G^{\ddagger}$ < 26.5 kJ/mol (6.3 kcal/mol). The drastic lowering of T_c and $\Delta G^{\ddagger}$, on going from the octaethyl-*N*,*N*′,*N*″,*N*‴-tetramethylisophlorin to tetraoxaisophlorin, is presumably due to the planar geometry of the latter as opposite to the saddle-like conformation of the former.[20] In this respect, it is worth mentioning that, in order to observe an analogous bond shift in the ^{13}C NMR spectra of heptalene, the solution must be cooled down to T_c = 113 K.[23] Presumably, a temperature well below 138 K is likewise necessary to detect this phenomenon in the NMR spectra of tetraoxaisophlorin, a requirement which can hardly be met in fluid solution, considering the poor solubility of the compound and the restricted choice of suitable solvents.

Supplementary Material Available: Figure S1 showing transitions between the SCF MO's of the five tetraoxaporphyrin redox stages as determined by PPP calculations starting from a perturbed D_{4h} geometry[8] (it corresponds to Figure 2 in the paper), Figure S2 displaying the SCF CI energy levels of the ground and relevant excited states resulting from these calculations, Table SI listing the characteristics of the pertinent electronic transitions[12] (3 pages). Ordering information is given on any current masthead page.

(19) Dewar, M. J. S.; Thiel, W. *J. Am. Chem. Soc.* **1977**, *99*, 4899, 4907.
(20) Pohl, M.; Schmickler, H.; Lex, J.; Vogel, E. *Angew. Chem., Int. Ed. Engl.* **1991**, *30*, 1693.
(21) See. e.g.: Günther, H. *NMR-Spektroskopie*, 2nd ed.; G. Thieme Verlag: Stuttgart–New York, 1983; p 229.
(22) The difference $\delta\nu$ = 120 Hz has been observed in the ^{1}H NMR spectrum of 5,10-dihydrotetraoxaisophlorin for protons in the furan moieties which are structurally similar to those in the double-bond-localized tetraoxaisophlorin. (The dihydro derivative is a precursor in the synthesis of the parent compound.[4])
(23) Vogel, E.; Königshofen, H.; Wassen, J.; Müllen, K.; Oth, J. F. M. Unpublished results, quoted as ref 16 in: Vogel, E.; Königshofen, H.; Müllen, K.; Oth, J. F. M. *Angew. Chem., Int. Ed. Engl.* **1974**, *13*, 281.

Synthesis and Vibrational Analysis of a Locked 14-*s-cis* Conformer of Retinal

Mary E. M. Cromwell,[1a,c] Ronald Gebhard,[1b,d] Xiao-Yuan Li,[1a,e] Elvira S. Batenburg,[1b] Johan C. P. Hopman,[1b] Johan Lugtenburg,[1b] and Richard A. Mathies*,[1a]

Contribution from the Departments of Chemistry, University of California, Berkeley, California 94720, and Leiden University, 2300 RA Leiden, The Netherlands.
Received April 29, 1992

Abstract: A 12-*N*-ethano retinal Schiff base is synthesized to study the vibrational properties of a C_{14}–C_{15} *s-cis* conformer of retinal. The synthesis of the 12-*N*-ethano retinal Schiff base and seven of its isotopomers is described. Raman and FTIR spectra of this compound and its isotopic derivatives are analyzed and the normal mode assignments compared to MNDO normal coordinate calculations. The frequency of the C_{14}–C_{15} stretch at 1096 cm^{-1} is ~100 cm^{-1} below typical values for *s-trans* conformers of retinal polyenes, supporting previous arguments that *s-cis* conformers will have characteristically low frequencies for the C–C stretch of the *s-cis* bond (Smith et al., *Proc. Natl. Acad. Sci. U.S.A.* **1986**, *83*, 967–971). Deuteriation at the 15-position produces two modes at 950 and 1044 cm^{-1} that contain C_{15}D rock character. The elevated frequency (1044 cm^{-1}) of the high-frequency component is a marker band for the C=N *syn* geometry and confirms an earlier analysis of the sensitivity of the C_{15}D rock frequency to Schiff base configuration (Ames et al., *Biochemistry* **1989**, *28*, 3681–3687). This work on retinals with chemically defined configuration and conformation provides a basis for further analysis of the geometry of these bonds in retinal-containing pigments.

Introduction

Retinal is the chromophore in visual pigments and in the light-transducing proteins found in halobacteria. Optical excitation of these pigments initiates a photochemical *cis–trans* double-bond isomerization of the retinal prosthetic group that occurs on a femtosecond time scale.[2,3] In visual pigments, this photoisomerization initiates an enzymatic cascade[4] that ultimately causes

(1) (a) University of California, Berkeley. (b) Leiden University. (c) Present address: Genentech, Inc., 460 Point San Bruno Blvd., South San Francisco, CA 94080. (d) Present address: Organon Int. B.V., P.O. Box 20, 5340 B.H. Oss, The Netherlands. (e) Present address: Department of Chemistry, The Hong Kong University of Science and Technology, Clear Water Bay, Kowloon, Hong Kong.
(2) Mathies, R. A.; Brito Cruz, C. H.; Pollard, W. T.; Shank, C. V. *Science* **1988**, *240*, 777–779.
(3) Schoenlein, R. W.; Peteanu, L. A.; Mathies, R. A.; Shank, C. V. *Science* **1991**, *254*, 412–415.

0002-7863/92/1514-10860$03.00/0 © 1992 American Chemical Society

Scheme I. Synthesis of the 12-*N*-Ethanoretinal Schiff Base **1**

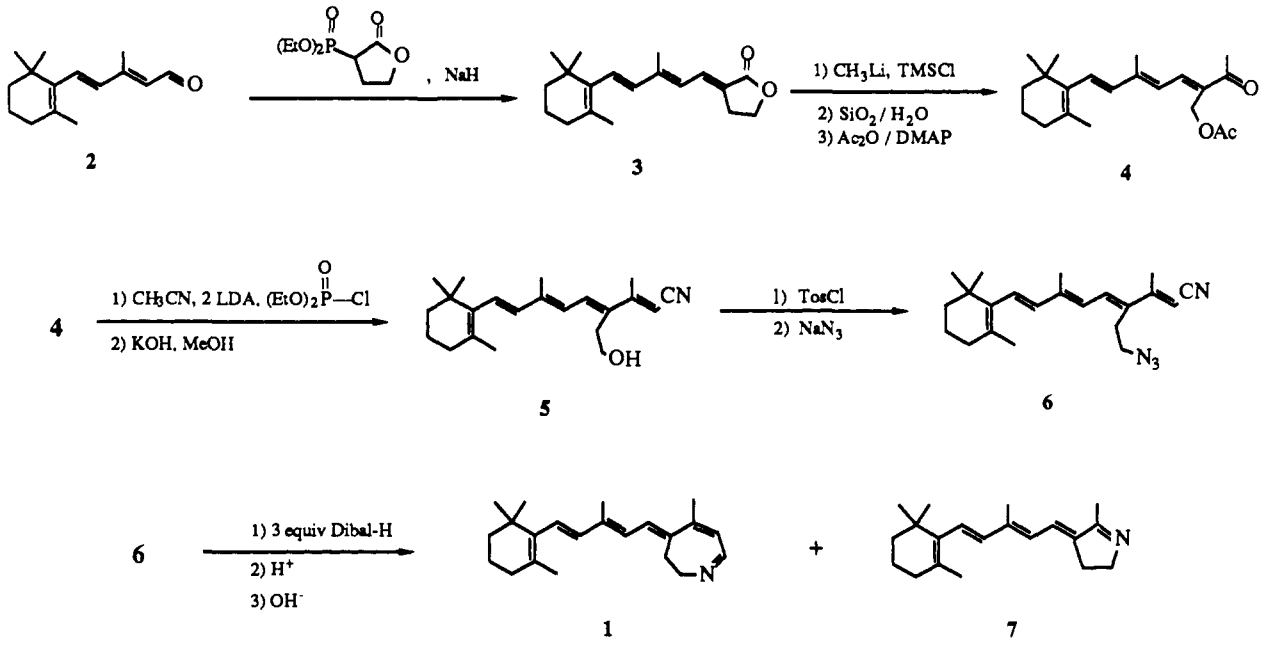

the photoreceptors to hyperpolarize. In the halobacteria pigments, the photoisomerization activates transmembrane ion pumps (bacteriorhodopsin and halorhodopsin) as well as several sensory pigments.[5,6] There is a great deal of interest in understanding the molecular mechanism of these phototransducing proteins.

This study is concerned with the development of a molecular understanding of the photochemistry in bacteriorhodopsin (BR). BR is a 26-kD transmembrane protein found in the purple membrane of *Halobacterium halobium*.[5,7,8] Upon light absorption, BR pumps a proton across the cell membrane, and the resulting proton gradient drives the synthesis of ATP.[9,10] The *all-trans* retinal prosthetic group in light-adapted BR_{568} is attached to the protein via a protonated Schiff base linkage to lysine 216. A C_{13}=C_{14} *trans-cis* isomerization in the initial photochemical step is followed by thermal relaxation which leads to Schiff base deprotonation in the M_{412} intermediate (Figure 1). Reprotonation of the Schiff base linkage occurs in N_{520} followed by reisomerization back to *all-trans* in O_{640}. A variety of molecular mechanisms linking the chromophore structure in the various intermediates to a mechanism of proton transport through the membrane have been presented.[7,11,12]

Vibrational spectroscopy is an important tool for determining the in situ chromophore structure in rhodopsins.[13] Analyses of the retinal isomers[14] and of the retinal chromophore in light-adapted[15] and dark-adapted[16] bacteriorhodopsin have provided

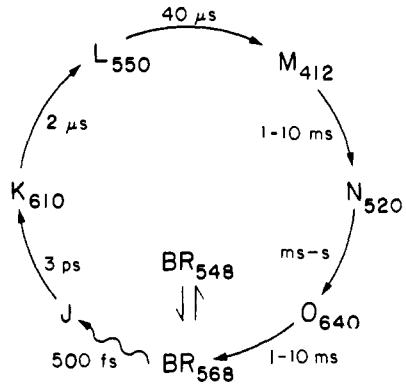

Figure 1. Photocycle of bacteriorhodopsin.

a detailed characterization of the vibrational structure of retinals as well as a number of useful methods for determining in situ chromophore structure. Recent vibrational work on BR has focused on the structure of the chromophore in the K_{610} and L_{550} intermediates.[17-21] While it is agreed that the chromophore undergoes a photoisomerization from *all-trans* to 13-*cis*, it has also been suggested that the primary photochemistry involves a 13-*trans*,14-*s-trans* to 13-*cis*,14-*s-cis* isomerization.[22-25] A number of vibrational studies have been performed to examine the C_{14}–C_{15} conformation in the K_{610} and L_{550} intermediates.[17,19-21,26] The

(4) Stryer, L. *Annu. Rev. Neurosci.* **1986**, *9*, 87–119.
(5) Stoeckenius, W.; Bogomolni, R. A. *Annu. Rev. Biochem.* **1982**, *51*, 587–616.
(6) Spudich, J. L.; Bogomolni, R. A. *Annu. Rev. Biophys. Biophys. Chem.* **1988**, *17*, 193–215.
(7) Mathies, R. A.; Lin, S. W.; Ames, J. B.; Pollard, W. T. *Annu. Rev. Biophys. Biophys. Chem.* **1991**, *20*, 491–518.
(8) Birge, R. R. *Biochim. Biophys. Acta* **1990**, *1016*, 293–327.
(9) Lozier, R. H.; Bogomolni, R. A.; Stoeckenius, W. *Biophys. J.* **1975**, *15*, 955–962.
(10) Racker, E.; Stoeckenius, W. *J. Biol. Chem.* **1974**, *249*, 662–663.
(11) Braiman, M. S.; Mogi, T.; Marti, T.; Stern, L. J.; Khorana, H. G.; Rothschild, K. J. *Biochemistry* **1988**, *27*, 8516–8520.
(12) Henderson, R.; Baldwin, J. M.; Ceska, T. A.; Zemlin, F.; Beckmann, E.; Downing, K. H. *J. Mol. Biol.* **1990**, *213*, 899–929.
(13) Mathies, R. A.; Smith, S. O.; Palings, I. In *Biological Applications of Raman Spectroscopy*: Vol. 2. *Resonance Raman Spectra of Polyenes and Aromatics*; Spiro, T. G., Ed.; John Wiley: New York, 1987; Vol. 2, pp 59–108.
(14) Curry, B.; Palings, I.; Broek, A. D.; Pardoen, J. A.; Lugtenburg, J.; Mathies, R. *Adv. Infrared Raman Spectrosc.* **1985**, *12*, 115–178.
(15) Smith, S. O.; Braiman, M. S.; Myers, A. B.; Pardoen, J. A.; Courtin, J. M. L.; Winkel, C.; Lugtenburg, J.; Mathies, R. A. *J. Am. Chem. Soc.* **1987**, *109*, 3108–3125.
(16) Smith, S. O.; Pardoen, J. A.; Lugtenburg, J.; Mathies, R. A. *J. Phys. Chem.* **1987**, *91*, 804–819.
(17) Smith, S. O.; Hornung, I.; van der Steen, R.; Pardoen, J. A.; Braiman, M. S.; Lugtenburg, J.; Mathies, R. A. *Proc. Natl. Acad. Sci. U.S.A.* **1986**, *83*, 967–971.
(18) Tavan, P.; Schulten, K. *Biophys. J.* **1986**, *50*, 81–89.
(19) Gerwert, K.; Siebert, F. *EMBO J.* **1986**, *5*, 805–811.
(20) Fodor, S. P. A.; Pollard, W. T.; Gebhard, R.; van den Berg, E. M. M.; Lugtenburg, J.; Mathies, R. A. *Proc. Natl. Acad. Sci. U.S.A.* **1988**, *85*, 2156–2160.
(21) Fahmy, K.; Siebert, F.; Grossjean, M. F.; Tavan, P. *J. Mol. Struct.* **1989**, *214*, 257–288.
(22) Liu, R.; Mead, D.; Asato, A. *J. Am. Chem. Soc.* **1985**, *107*, 6609–6614.
(23) Schulten, K.; Tavan, P. *Nature (London)* **1978**, *272*, 85–86.
(24) Orlandi, G.; Schulten, K. *Chem. Phys. Lett.* **1979**, *64*, 370–374.
(25) Schulten, K.; Schulten, Z.; Tavan, P. In *Information and Energy Transduction in Biological Membranes*; A. R. Liss, Inc.: New York, 1984; pp 113–131.
(26) Grossjean, M. F.; Tavan, P.; Schulten, K. *J. Phys. Chem.* **1990**, *94*, 8059–8069.

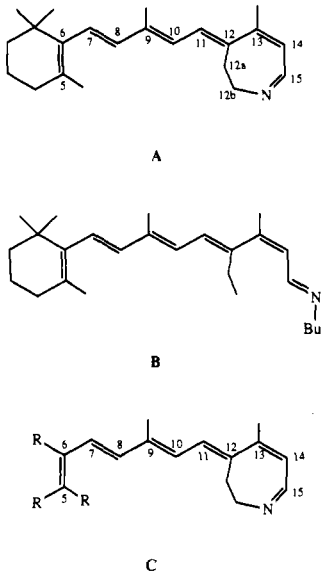

Figure 2. Structures of the 12-*N*-ethano retinal Schiff base (A) and the 13-*cis*-12-ethyl Schiff base (B). C is the abbreviated structure used in the MNDO calculations.

location of the C_{14}–C_{15} stretching mode first suggested that the chromophore in K_{610} and L_{550} was 14-*s-trans*.[17] Subsequently, an analysis of the deuteriated rocking mode frequencies in pigments regenerated with 14,15-dideuterio retinals provided additional evidence for the 14-*s-trans* conformation.[20] Calculations indicate that the coupling between the C_{14}–D and C_{15}–D rocking modes is negligible in the 14-*s-trans* conformation so that the deuteriated rocks are both found at 970 cm^{-1}. In the 14-*s-cis* conformation, the two rocking coordinates are predicted to be strongly coupled, producing modes of A and B symmetry near 860 cm^{-1} and 1015 cm^{-1}, respectively. Experimentally, the A symmetry Raman-active mode is found at 963 cm^{-1} in L_{550}, 958 cm^{-1} in M_{412}, and 966 cm^{-1} in N_{520} as expected for the 14-*s-trans* structure.[20,27]

Vibrational data on a retinal model compound with a chemically defined C_{14}–C_{15} *s-cis* structure would be valuable in providing more spectroscopic data on these unusual *s-cis* polyenes. Toward this end we have synthesized a 12-*N*-ethano retinal Schiff base (structure A in Figure 2) that is locked in the 14-*s-cis*, C=N *syn* conformation. The spectra and vibrational analysis presented here provide the first data on a retinal model compound of known C_{14}–C_{15} conformation. Vibrational assignments are developed from data on a series of deuteriated and ^{13}C-labeled compounds. These assignments are extended and analyzed through MNDO normal coordinate calculations. This work extends our knowledge of retinal vibrational structure to the properties of unstable conformers. This knowledge should be valuable in the further exploration of the molecular mechanisms of retinal proteins.

Synthetic Methods. The synthesis of 12-*N*-ethano retinylimine (**1**) is performed according to Scheme I. In the first step, β-ionylideneacetaldehyde (**2**), easily accessible from β-ionone,[28] is converted in a Horner–Wadsworth–Emmons (HWE) reaction with 2-(diethylphosphono)-4-butyrolactone[29] and sodium hydride as a base to the unsaturated lactone **3**. The reaction proceeds with 100% *E* selectivity and gives, after purification, **3** in 96% yield. For the conversion of the lactone **3** into the corresponding acetoxy ketone **4**, **3** is first treated with 1.5 equiv of methyllithium in the presence of 5 equiv of trimethylsilyl chloride (TMSCl).[30] After workup and esterification, acetoxy ketone **4** was obtained in 71% yield based on **3**. The extension of **4** to the required 12-substituted retinonitrile **5** is effected by a HWE reaction with diethyl cyanomethylphosphonate (C_2-phosphonate), using lithium diisopropylamide (LDA) as a base. Owing to steric hindrance, only the 13-*E* isomer is obtained. The C_2-phosphonate was prepared quantitatively in situ from acetonitrile (1 equiv), LDA (2 equiv), and diethyl chlorophosphate (1 equiv).[31] This is very convenient, since it allows the introduction of ^{13}C on C_{14} and C_{15} or ^2H on C_{14} by using the appropriately labeled acetonitrile.[32,33] The resulting acetoxy nitrile has the complete carbon skeleton of **1**. To obtain the cyclic imine **1**, the acetoxy group has to be converted into an amine function, the nitrile to an aldehyde, and the 13-*E* double bond to a 13-*Z* double bond to allow an intramolecular ring closure. In order to achieve the conversion of the acetoxy group into a nitrogen function, first the acetoxy function is saponified with KOH/methanol at −20 °C, giving hydroxy nitrile **5**. At room temperature, the saponification is followed by an efficient intramolecular base-catalyzed 1,4-addition, yielding the corresponding furano nitrile derivative. The primary hydroxyl function is subsequently converted via the tosylate (*p*-TosCl, pyridine, 75%) into the corresponding azide (NaN_3, DMF, 95%), thus yielding the azido nitrile **6**. The conversion of **6** into the desired seven-membered ring imine **1** is performed in a one-pot procedure. Treating azido nitrile **6** at −60 °C with excess (3 equiv) Dibal-H and warming the mixture to room temperature result in the reduction of the nitrile function to an aldehyde and of the azido group to an amino function. It appears that the product composition is critically dependent on the pH during the hydrolysis step: hydrolysis at pH 4, followed by neutralization with aqueous NaOH solution, mainly gives the five-membered ring imine **7** plus traces of the desired seven-membered ring imine **1**. Most likely **7** has been formed by an intramolecular Michael addition of the amino function of the intermediate amino aldehyde on the conjugated aldehyde system followed by an acid-catalyzed retro–aldol condensation. When the pH during hydrolysis is kept between 5.5 and 6.5, up to 50% of the seven-membered ring imine **1** is formed. Evidently, under these milder conditions an efficient acid-catalyzed *trans–cis* isomerization of the 13,14-double bond followed by seven-membered ring formation takes place. By carrying out the hydrolysis procedure in the presence of 3-Å molecular sieves, an optimal formation of the seven-membered ring system **1** is obtained (80% of the total amount). HPLC analysis (5:5:1 v/v, ether/petroleum ether/methanol eluent) of the reaction mixture showed four peaks. The most prominent peak (retention time 9.5 min) belongs to the desired 7*E*,9*E*,11*E* isomer of **1**. The other peaks belong to the 7*E*,9*Z*,11*E* (11.3 min) and the 7*E*,9*E*,11*E* and the 7*E*,9*Z*,11*E* isomers of **7**. The 7*E*,9*E*,11*E* isomer of **1** has been obtained in pure form by preparative HPLC. The yield of **1** is 30% based on azido nitrile **6**.

The (14-^{13}C), (15-^{13}C), (14,15-$^{13}C_2$), and 14-^2H isotopomers of **1** have been prepared with high isotope incorporation according to Scheme I by using the appropriately labeled acetonitrile in the conversion of **4** to **5**. Thus, (14-^{13}C)imine **1a** is obtained from (2-^{13}C)acetonitrile in an overall yield of 16%; similarly, (1-^{13}C)acetonitrile gave (15-^{13}C)**1b** and (1,2-$^{13}C_2$)acetonitrile led to (14,15-$^{13}C_2$)-labeled **1c**. For the preparation of (14-^2H)**1d**, we used CD_3CN. The most efficient method for the introduction of the ^2H atom at C_{15} is treating **6** with Dibal-^2H. We have prepared pure Dibal-^2H according to a published procedure,[34] and diluted it to a 1 M solution in hexane (CAUTION: pure Dibal-^2H is a pyrophoric liquid!). Reduction of azidonitrile **6** with 3 equiv of Dibal-^2H, furnished after workup the 15-^2H labeled imine **1e**; similarly, reduction of (14-^2H)-labeled **6** afforded the 14,15-dideuteriated imine **1f** and reduction of (14,15-$^{13}C_2$)-labeled **6** gives the (14,15-$^{13}C_2$,15-^2H)-labeled **1g**.

(27) Ames, J. B.; Fodor, S. P. A.; Gebhard, R.; Raap, J.; van den Berg, E. M. M.; Lugtenburg, J.; Mathies, R. A. *Biochemistry* **1989**, *28*, 3681–3687.
(28) Dugger, R. W.; Heathcock, C. H. *Synth. Commun.* **1980**, *10*, 509–515.
(29) Büchel, K. A.; Rochling, H.; Korte, F. *Justus Liebigs Ann. Chem.* **1965**, *685*, 10–15.
(30) Cooke, M. P., Jr. *J. Org. Chem.* **1986**, *51*, 951–953.
(31) Comins, D. L.; Jacobine, A. F.; Marshall, J. L.; Turnbull, M. M. *Synthesis* **1978**, 309–311.
(32) Gebhard, R.; van der Hoef, K.; Lefeber, A. W. M.; Erkelens, C.; Lugtenburg, J. *Recl. Trav. Chim. Pays-Bas* **1990**, *109*, 378–387.
(33) Gebhard, R.; van Dijk, J. T. M.; Boza, M. V. T. J.; van der Hoef, K.; Lugtenburg, J. *Recl. Trav. Chim. Pays-Bas* **1991**, *110*, 332–341.
(34) Goerger, M. M.; Hudson, B. S. *J. Org. Chem.* **1988**, *53*, 3148–3153.

The synthesis of 12-ethylretinal has been described.[35] Irradiation of the *all-trans* isomer in acetonitrile gives a *cis/trans* isomeric mixture from which the 13-*cis* isomer can be separated with HPLC. The Schiff base (structure B in Figure 2) was formed by dissolving ~0.5 mg of the retinal in 1 mL of ether with 40 μL of *n*-butylamine for 30 min in the presence of 4-Å molecular sieves. The ether and *n*-butylamine were then evaporated, and the Schiff base residue was dissolved in the appropriate solvent (hexane or carbon tetrachloride) to obtain either the FTIR or the Raman spectrum.

Spectroscopic Methods. Raman spectra were obtained from a stationary chloroform solution with 25–50 mW of 752.4-nm excitation focused onto the sample with a 75-mm lens. Raman data were acquired with a Spex 1401 double monochromator equipped with photon-counting detection. The spectral slit width was ~4 cm^{-1}, the monochromator step size was 2 cm^{-1}, and the scan dwell time was 2 s. Spectra are averages of 6 to 20 scans and were corrected for detector sensitivity. A chloroform spectrum and a fluorescence background, simulated by a quartic polynomial, were subtracted from the averaged spectra.

Infrared spectra were obtained from thin films formed by evaporating a hexane solution of the Schiff base on KBr windows. Infrared data were collected on a Nicolet 5DX FTIR. Data reported here are averages of 10 to 100 scans with 2-cm^{-1} resolution.

Computational Methods. Normal mode calculations were performed on the Schiff base chromophore (structure C in Figure 2) using the MNDO method.[36] R groups have a mass of 15 and the parameters of an sp^3 carbon. The starting geometries used in the MNDO calculation were generated by a QCFF/PI calculation.[37] All geometric parameters (bond angles, bond lengths, and dihedral angles) were minimized. The force field was then calculated on the minimized geometry. The frequencies were calculated using the MNDO Hamiltonian and spectroscopic masses previously shown necessary to obtain reasonable results.[21] Normal modes were identified as a particular stretch or rock, etc., by finding those modes that contained the highest component of the relevant internal coordinate. This is often difficult since the internal coordinate character can be spread over many normal modes (e.g., see Table I). MNDO calculations were performed on the seven-membered ring chromophore and on an unlocked, planar 13-*cis*, 14-*s-cis*, C=N *syn* chromophore to determine the effect of nonplanarity on the normal modes. The basic normal mode frequency and coupling pattern were found to be the same in both molecules.

Results and Discussion

Effect of Ring Formation. To form a covalent C_{14}–C_{15} *s-cis* retinal, it is necessary to substitute the chromophore at C_{12}. To understand the vibrational consequences of this substitution, we first synthesized molecules with an ethyl group at C_{12} but no cyclic ring (structure B in Figure 2). Figure 3 presents a comparison of the Raman spectra of the 13-*cis* Schiff base, the 12-ethyl,13-*cis* Schiff base, and the 12-*N*-ethano Schiff base. The normal mode assignments of the 13-*cis* Schiff base have been determined using isotopic substitution.[16] The assignment of the 12-ethyl retinal is based on analogy with these previous assignments. Although the intensities of the fingerprint lines for the 12-ethyl,13-*cis* Schiff base are significantly different from those of the 13-*cis* Schiff base, the frequency pattern corresponds well. Resonance Raman intensities are often more sensitive than mode frequencies to subtle changes in normal mode character. The 1224-cm^{-1} mode in the 13-*cis* Schiff base is the "C_{12}–C_{13} stretch". The C_{12}–C_{13} stretch is expected to shift up slightly upon substitution at C_{12}[14] so the intense 1228-cm^{-1} band in 12-ethylretinal is assigned as the C_{12}–C_{13} stretch. The 1199-cm^{-1} line in the 13-*cis* Schiff base is the C_8–C_9 stretch. The close correspondence of this mode with

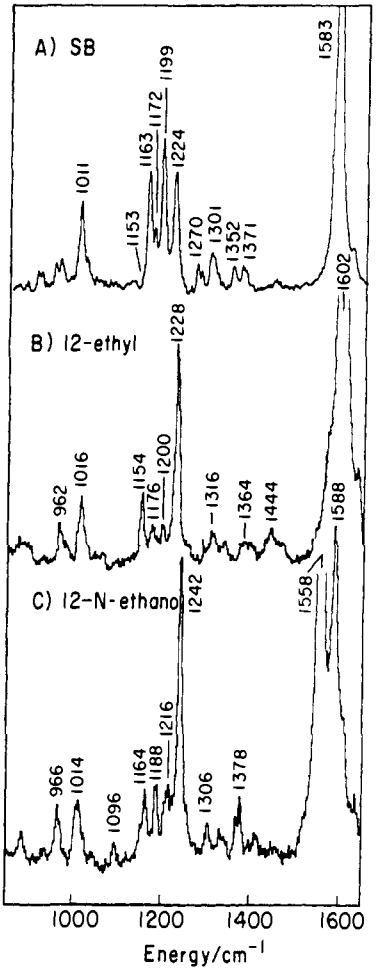

Figure 3. Raman spectra of (A) 13-*cis*-retinal Schiff base,[16] (B) 12-ethyl,13-*cis* Schiff base, and (C) 12-*N*-ethano Schiff base.

the 1200-cm^{-1} mode in the 12-ethyl derivative argues that this is the C_8–C_9 stretch. The weak 1172-cm^{-1} band in the 13-*cis* Schiff base is the C_6–C_7 stretch[14] which is expected to be unaffected by the modifications introduced here. The C_{14}–C_{15} stretch is assigned at 1153 cm^{-1} in the 13-*cis* Schiff base spectrum based on its infrared intensity.[16] The enhanced polarity of the C_{14}–C_{15} bond in retinals typically makes the C_{14}–C_{15} stretch the strongest C–C mode in the IR spectrum.[14] In the 12-ethyl derivative this mode shifts up to 1172 cm^{-1} (IR) or 1176 cm^{-1} (Raman) based on the intensity of this line in the IR (see below). The C_{10}–C_{11} stretch is found at 1163 cm^{-1} in the 13-*cis* Schiff base. Correspondence suggests that the 1154-cm^{-1} mode in the 12-ethyl derivative is the C_{10}–C_{11} stretch. Thus, the only significant change in the vibrational pattern of the ethyl-substituted Schiff base is the upshift of the C_{14}–C_{15} mode to 1176 cm^{-1} (Raman). The other modes are readily identified by analogy to the unsubstituted compound.

Figures 4 and 5 present the complete Raman and FTIR spectra of the 12-ethyl,13-*cis* retinal Schiff base and the 12-*N*-ethano retinal Schiff-base derivatives. Comparing the spectra of the 12-ethyl Schiff base and the 12-*N*-ethano Schiff base yields information about the effect of ring formation on the vibrational pattern. The infrared spectra (Figure 5, A and B) show that the line at 1172 cm^{-1} shifts down to 1091 cm^{-1} when the ring is formed. Inspection of the Raman spectra (Figure 3, B and C) reveals that a weak line appears at 1096 cm^{-1} in the 12-*N*-ethano retinal. This line will be assigned as the C_{14}–C_{15} stretch. The intense C_{12}–C_{13} stretch shifts to 1242 cm^{-1} in the 12-*N*-ethano derivative (Figure 3C). A line appears at 1164 cm^{-1} in the ring-closed species that is assigned as the C_{10}–C_{11} stretch. Finally, the C_8–C_9 stretch appears to be split into modes at 1188 and 1216 cm^{-1}. This splitting may result from coupling with the single bond stretches in the ring or from coupling with CH_2 modes. The detailed arguments leading to these assignments are presented below.

(35) Groesbeek, M.; van der Steen, R.; van Vliet, J. C.; Vertegaal, L. B. J.; Lugtenburg, J. *Recl. Trav. Chim. Pays-Bas* **1989**, *108*, 427–436.
(36) Dewar, M. J. S.; Thiel, W. *J. Am. Chem. Soc.* **1977**, *99*, 4899–4907.
(37) Warshel, A.; Karplus, M. *J. Am. Chem. Soc.* **1974**, *96*, 5677–5689.

Table I. Calculated Normal Modes for Locked 14-*s-cis*-Retinal[a]

Derivative	Frequency (cm^{-1})	Assignment
native	979	- 0.53 CCH(20Me)s + 0.28 w(15H) + 0.22 w(CbH2) - 0.20 w(14H) + 0.13r(12-13-14) + 0.13 s(14-15)
	1060	0.63 CCH(20Me)s + 0.20 CCH(20Me)a + 0.18 r(20C) - 0.17 r(14H) + 0.15 w(CbH2) + 0.13 CCH(19Me)a + 0.11 r(CeH2) + 0.10 s(14-15)
	1190	- 0.18 r(15H) + 0.12 r(CeH2) - 0.11 r(10H) + 0.10 s(13-20) - 0.10 s(14-15) - 0.09 w(Cb)
	1203	0.56 twi(CeH2) - 0.31 r(10H) + 0.28 r(15H) + 0.22 r(11H) - 0.17 twi(CbH2) + 0.16 r(CbH2) + 0.14 CCH(20Me)s - 0.12 t(Ce-Cb) - 0.12 s(N-Ce) - 0.12 b(8-9-10)
14D	887	0.66 r(14H) + 0.20 w(15H) - 0.15 w(11H) - 0.10 w(14H) + 0.09 w(CeH2) - 0.08 s(14-15) - 0.07 s(N-Ce)
	934	1.01 w(15H) - 0.39 w(14H) - 0.38 w(10H) - 0.19 r(14H) + 0.17 w(CbH2) - 0.12 w(11H)
	991	0.58 CCH(20Me)s - 0.39 r(14H) + 0.32 CCH(20Me)a + 0.15 w(CeH2) + 0.11 w(10H) - 0.09 w(15H) - 0.07 s(N-Ce)
	1090	- 0.34 CCH(20Me)s - 0.30 r(14H) - 0.19 w(CbH2) + 0.18 CCH(19Me)a + 0.17 r(R1) - 0.15 CCH(20Me)a - 0.15 w(7H)
	1090	0.31 CCH(20Me)s + 0.27 r(14H) + 0.20 r(R1) + 0.16 w(CbH2) - 0.16 s(6-R3) - 0.15 w(7H) - 0.14 r(R3)
	1121	- 0.20 r(14H) + 0.19 s(Ce-Cb) - 0.16 CCH(20Me)s + 0.13 w(CeH2) + 0.10 r(CbH2)
	1165	0.18 s(13-20) + 0.13 r(11H) - 0.13 r(CeH2) - 0.12 w(CeH2) + 0.12 r(12-13-14) + 0.12 s(Ce-Cb) - 0.12 r(14H)
	1191	0.15 r(15H) - 0.13 s(13-20) + 0.12 r(14H) + 0.11 s(14-15) - 0.10 r(CeH2) + 0.10 w(Cb)
	1206	0.39 r(10H) - 0.28 r(15H) - 0.21 r(11H) - 0.16 CCH(20Me)s - 0.14 r(14H) - 0.14 r(7H)
15D	704	- 0.66 w(15H) - 0.25 w(14H) - 0.10 r(15H)
	727	0.60 w(15H) + 0.16 w(14H) - 0.12 r(15H)
	852	0.39 w(CbH2) + 0.26 w(11H) - 0.23 w(10H) - 0.23 w(CeH2) + 0.21 r(15H) - 0.12 w(Cb)
	868	0.53 w(11H) - 0.47 w(10H) + 0.22 w(CeH2) - 0.20 r(15H) - 0.16 w(CbH2) - 0.12 w(Cb)
	900	0.48 r(15H) - 0.34 w(8H) - 0.31 w(7H) - 0.26 w(10H) + 0.21 w(CeH2)
	906	- 0.86 w(8H) - 0.82 w(7H) + 0.20 w(R3) - 0.18 r(15H) - 0.10 w(CeH2) - 0.07 w(R2)
	936	- 0.69 w(10H) - 0.22 CCH(19Me)a - 0.20 r(15H) + 0.19 w(11H) + 0.14 w(19C) - 0.13 s(9-19)
	968	- 0.42 CCH(20Me)s - 0.22 CCH(20Me)a - 0.17 w(10H) - 0.14 w(CeH2) + 0.12 s(14-15) - 0.10 w(14H) + 0.10 s(N-Ce) + 0.10 r(15H)
	1008	- 0.47 w(CbH2) - 0.45 w(CeH2) + 0.23 r(15H) - 0.17 w(10H) + 0.16 CCH(19Me)s + 0.15 CCH(19Me)a - 0.14 r(Cb)
	1018	0.67 CCH(19Me)a + 0.40 CCH(19Me)s + 0.19 w(11H) - 0.18 r(15H) + 0.16 w(CbH2) + 0.10 w(CeH2) + 0.09 r(19C) - 0.08 w(8H)
	1030	0.68 CCH(19Me)s - 0.37 CCH(19Me)a - 0.25 CCH(20Me)a - 0.23 w(19C) + 0.22 r(15H) + 0.21 CCH(20Me)s - 0.16 w(14H) + 0.10 w(CeH2)
	1032	- 0.48 CCH(20Me)a - 0.40 CCH(19Me)s + 0.38 CCH(20Me)s + 0.30 CCH(19Me)a - 0.29 w(14H) + 0.29 r(15H) - 0.20 w(20C) + 0.17 w(19C)
	1040	- 0.65 CCH(20Me)a - 0.38 r(15H) - 0.24 w(14H) - 0.23 w(20C) - 0.17 w(Cb) - 0.14 CCH(19Me)a - 0.14 w(CeH2)
	1247	0.51 r(8H) + 0.50 r(7H) + 0.33 r(10H) + 0.32 r(15H) + 0.26 r(CeH2) + 0.25 r(14H) + 0.15 s(N-Ce) - 0.13 s(14-15) + 0.11 CCH(19Me)a
	1250	- 0.57 r(8H) - 0.52 r(7H) + 0.32 r(15H) + 0.26 r(CeH2) - 0.24 r(10H) - 0.21 r(11H) + 0.15 s(N-Ce) - 0.14 s(14-15) - 0.12 CCH(19Me)a
14,15-D_2	720	- 0.22 w(15H) + 0.16 r(15H) - 0.12 w(14H) - 0.11 w(CbH2)
	851	- 0.38 w(CbH2) - 0.27 w(11H) + 0.25 w(10H) + 0.23 w(CeH2) - 0.19 r(15H) + 0.12 w(Cb)
	867	0.51 w(11H) - 0.45 w(10H) + 0.24 w(CeH2) - 0.22 r(15H) - 0.19 w(CbH2) - 0.11 w(Cb)
	888	0.67 r(14H) - 0.13 w(11H) - 0.12 w(15H) + 0.08 w(CeH2) - 0.08 s(14-15) - 0.08 w(CbH2) + 0.07 w(14H) - 0.07 s(N-Ce)
	899	- 0.49 r(15H) + 0.31 w(8H) + 0.28 w(7H) + 0.27 w(10H) - 0.20 w(CeH2) + 0.12 CCH(20Me)s
	906	0.87 w(8H) + 0.83 w(7H) - 0.20 w(R3) + 0.17 r(15H) + 0.09 w(CeH2) + 0.07 w(R2)
	936	- 0.69 w(10H) - 0.22 CCH(19Me)a + 0.22 w(11H) - 0.18 r(15H) + 0.14 w(19C) - 0.13 s(9-19)
	989	0.60 CCH(20Me)s - 0.39 r(14H) + 0.32 CCH(20Me)a + 0.14 w(CeH2) - 0.07 w(10H) + 0.07 w(11H) - 0.07 s(14-15)
	1008	0.48 w(CbH2) + 0.46 w(CeH2) - 0.25 r(15H) + 0.18 w(10H) - 0.15 CCH(19Me)s - 0.14 CCH(20Me)a + 0.14 r(Cb)
	1018	0.67 CCH(19Me)a + 0.40 CCH(19Me)s + 0.20 w(11H) - 0.17 r(15H) + 0.15 w(CbH2) + 0.10 CCH(20Me)s + 0.09 r(19C) + 0.08 w(CeH2) - 0.08 w(8H)

Table I (Continued)

Derivative	Frequency (cm^{-1})	Assignment
	1027	0.71 CCH(20Me)a - 0.37 CCH(20Me)s - 0.28 r(15H) + 0.25 w(20C) + 0.18 w(14H) - 0.14 CCH(19Me)s
	1041	0.43 r(15H) + 0.40 CCH(20Me)a + 0.20 CCH(19Me)a - 0.19 CCH(20Me)s + 0.18 w(Cb) + 0.18 w(20C) + 0.17 s(Ce-Cb) + 0.16 w(CeH2)
	1092	0.46 CCH(20Me)s + 0.41 r(14H) + 0.22 CCH(20Me)a + 0.22 w(CbH2) + 0.18 r(20C) + 0.16 r(15H) + 0.12 r(11H) - 0.11 s(12-Cb)
	1122	- 0.24 r(14H) - 0.20 CCH(20Me)s + 0.16 s(Ce-Cb) + 0.12 w(CeH2) - 0.11 r(20C) + 0.09 r(CbH2)
	1164	0.20 s(13-20) + 0.16 r(11H) - 0.16 r(14H) - 0.12 w(CeH2) + 0.12 r(Cb) + 0.11 w(CbH2)
	1248	- 0.59 r(8H) - 0.56 r(7H) - 0.34 r(10H) - 0.30 r(15H) - 0.24 r(CeH2) + 0.13 s(14-15) - 0.13 s(N-Ce) - 0.13 CCH(19Me)a
	1250	0.52 r(8H) + 0.48 r(7H) - 0.32 r(15H) + 0.27 r(11H) - 0.27 r(CeH2) + 0.23 r(10H) + 0.15 s(14-15) - 0.15 s(N-Ce) + 0.11 CCH(19Me)a
14,15-^{13}C-15D	716	0.64 w(15H) + 0.15 w(14H) - 0.10 r(15H)
	851	- 0.38 w(CbH2) - 0.27 w(11H) + 0.25 w(10H) + 0.23 w(CeH2) - 0.20 r(15H) + 0.13 w(Cb)
	897	- 0.49 r(15H) + 0.26 w(10H) + 0.25 w(8H) - 0.22 w(CeH2) + 0.22 w(7H) + 0.11 CCH(20Me)s
	906	0.88 w(8H) + 0.84 w(7H) - 0.20 w(R3) + 0.19 w(14H) + 0.12 r(15H) + 0.08 w(CeH2)
	936	- 0.70 w(10H) - 0.22 CCH(19Me)a - 0.19 r(15H) + 0.17 w(11H) + 0.14 w(19C) - 0.13 s(9-19)
	1008	- 0.48 w(CbH2) - 0.45 w(CeH2) + 0.28 r(15H) - 0.19 w(10H) - 0.15 r(Cb) + 0.14 CCH(19Me)s
	1018	0.67 CCH(19Me)a + 0.40 CCH(19Me)s - 0.20 r(15H) + 0.20 w(11H) + 0.13 w(CbH2) + 0.09 r(19C) - 0.08 w(8H)
	1029	- 0.42 CCH(20Me)a + 0.38 CCH(19Me)s + 0.37 CCH(20Me)s + 0.36 r(15H) - 0.25 w(14H) - 0.17 w(20C) + 0.16 w(CeH2)
	1031	- 0.69 CCH(19Me)s + 0.46 CCH(19Me)a + 0.26 w(19C) - 0.25 CCH(20Me)a + 0.20 CCH(20Me)s - 0.15 w(10H) - 0.14 w(14H) + 0.13 r(15H)
	1038	- 0.70 CCH(20Me)a - 0.34 r(15H) - 0.24 w(20C) - 0.24 w(14H) - 0.16 w(Cb) - 0.15 CCH(19Me)a - 0.14 w(CeH2)
	1193	0.22 r(11H) - 0.17 r(10H) + 0.16 r(CbH2) + 0.11 r(15H) + 0.11 r(CeH2)

[a] Coefficients dS/dQ of symmetry coordinates S in the normal modes Q. Only coordinates with significant C_{14} or C_{15} character have been listed. In each coordinate, only the predominant components have been listed. Symbols used: s, symmetric stretch; a, asymmetric stretch; w, out-of-plane wag; r, in-plane rock; twi, twist; b, bend; t, torsion.

C_{14}–C_{15} Stretch. The C_{14}–C_{15} stretch should be sensitive to ^{13}C substitution at the 14 and 15 positions. The 1096-cm^{-1} line in the unlabeled molecule (Figure 6A) downshifts 6 cm^{-1} in each of the monolabeled compounds (Figure 6, B and C) and 12 cm^{-1} in the di-^{13}C-labeled molecule (Figure 6D). Correspondingly, the FTIR spectra of these compounds show that the moderately strong 1091-cm^{-1} line in the native molecule (Figure 5B) shifts 4 cm^{-1} in each of the mono-^{13}C-labeled compounds (Figure 5, G and H) and 8 cm^{-1} in the di-labeled compound (Figure 5I). The 1096-cm^{-1} (Raman) line in the native molecule is, therefore, confidently assigned as the C_{14}–C_{15} stretch. The position of this mode, ~80 cm^{-1} below its frequency in the 14-*s-trans* molecule, is consistent with the predicted reduction of the C_{14}–C_{15} stretch modes in *s-cis* conformers.[17]

MNDO calculations performed on the 14-*s-cis* locked molecule (Table I) predict modes containing significant C_{14}–C_{15} character at 979, 1060, and 1190 cm^{-1}. Only the 1060-cm^{-1} mode is predicted to be sensitive to substitution at both the C_{14} and C_{15} positions, shifting 2–3 cm^{-1} in each case (not shown). In the di-^{13}C compound, the 1060-cm^{-1} mode shifts to 1055 cm^{-1}. These shifts are on the order of those observed in the vibrational spectra confirming the assignment.

C=N Configuration. Based on studies of retinal Schiff bases, the C_{15}D rock is expected to appear at ~975 cm^{-1} in molecules that have the C=N *anti* configuration.[15,20,27,38] In molecules having the C=N *syn* configuration, the C_{15}D rock is strongly coupled with the N–C stretch producing two mixed modes at ~1040 and ~910 cm^{-1}.[27] The 12-*N*-ethano,13-*cis* Schiff base, which has a chemically locked C=N *syn* configuration, provides a test of this prediction. Comparing the Raman spectra of the 15-D derivative to that of the unlabeled compound (Figure 7, A and C), lines appear at 950 and 1044 cm^{-1}. In the infrared spectrum of the 15-D derivative (Figure 5D), a weak line appears at 1045 cm^{-1} along with a very weak shoulder at 949 cm^{-1}. The in-plane vinyl rocks of retinal compounds typically have little intrinsic infrared intensity unless they are mixed with the skeletal stretches. Thus, the infrared data are not inconsistent with the idea that these two modes contain C_{15}D rock character. In the Raman spectrum of the 14,15-di-^{13}C,15D derivative (Figure 7E), these lines shift to ~940 and ~1030 cm^{-1}. The observation that both lines shift indicates that both modes also contain significant C_{14}–C_{15} stretch character. This is consistent with the infrared data on the 14,15-di-^{13}C,15D compound (Figure 5E) in which the mode at 1045 cm^{-1} loses intensity relative to the mode at 1028 cm^{-1}. The high frequency of the 1044-cm^{-1} C_{15}D rock component as well as its sensitivity to placement of ^{13}C at the 14- and 15-positions is analogous to previous vibrational results on the 13-*cis*,C=N *syn* chromophore in dark-adapted BR and completely consistent with the predictions of previous Wilson FG and QCFF-π calculations[27] on the vibrational properties of C=N *syn* retinal chromophores. These previous calculations argued that the C_{15}D rock would couple strongly with the N–C_{lys} stretch, producing two mixed modes at ~1040 and ~910 cm^{-1} as seen here. The 1044-cm^{-1} and the 950-cm^{-1} line in the 15D derivative are, therefore, assigned as the C_{15}D rock ± N–C stretch. These observations on a retinal model compound having a chemically defined structure strongly support the arguments presented in Ames et al.,[27] indicating that the C_{15}D rock is a good marker band for C=N configuration in retinal Schiff bases.

The C_{15}D rock is calculated to be coupled with the methyl rock, C_{14}–C_{15} stretch, N–C stretch, ring C–C stretch, C_{14}H wag, and C_{11}H wag with its character distributed among several modes between 852 and 1040 cm^{-1} (Table I). The predominant C_{15}D rock character is split between the 1040- and 900-cm^{-1} modes, which correspond reasonably well with the observed frequencies.

(38) Massig, G.; Stockburger, M.; Gärtner, W.; Oesterhelt, D.; Towner, P. *J. Raman Spectrosc.* **1982**, *12*, 287–294.

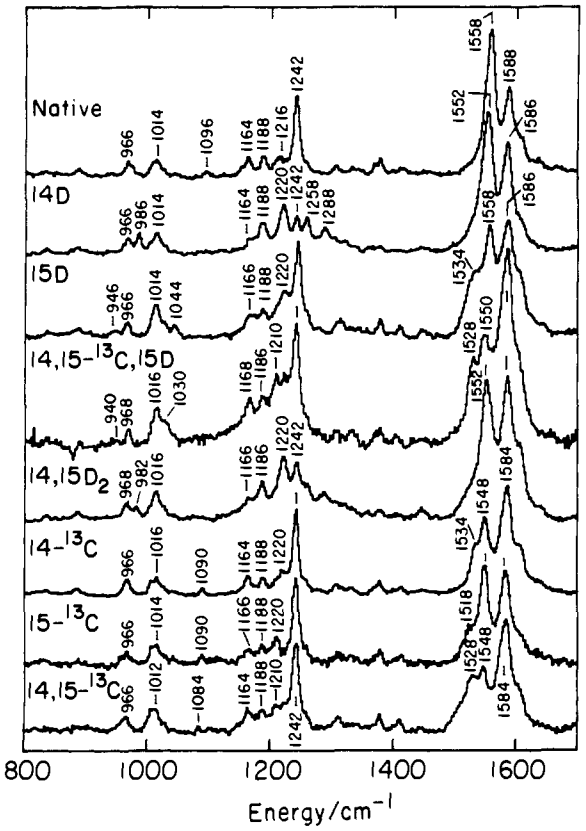

Figure 4. Raman spectra of the 12-*N*-ethano retinal Schiff base and its 14D, 15D, 14,15-^{13}C,15D, 14,15D$_2$, 14^{13}C, 15^{13}C, and 14,15-^{13}C derivatives. All Raman spectra were obtained using a stationary chloroform solution with 25–50 mW of spherically focused 752.4-nm excitation.

However, the MNDO calculation does not reproduce the expected mixing of the $C_{15}D$ rock with the N–C_{15} and the C_{14}–C_{15} stretches as well as our previous calculations.[27]

$C_{14}D$ and $C_{15}D$ Rocks. The coupling between the $C_{14}D$ rock and the $C_{15}D$ rock in the 14,15-dideuteriated compound is sensitive to the conformation about the C_{14}–C_{15} bond.[20] In the 14-*s-trans* conformation, the two rocks are only weakly coupled and are both found at ~970 cm^{-1}. In the 14-*s-cis* conformation, the two rocks are predicted to be strongly coupled with the modes of A and B symmetry split by ~160 cm^{-1}. The monodeuterio and dideuterio Raman data are presented in Figure 7. Comparison in Figure 7 of A and B reveals that a mode appears at 986 cm^{-1} in the 14D derivative with no corresponding infrared intensity (Figure 5C). This mode is assigned as the $C_{14}D$ rock. As presented earlier, the $C_{15}D$ rock is split into two modes at 950 and 1044 cm^{-1}, each with weak infrared intensity but significant Raman intensity. In the 14,15-dideuteriated compound (Figure 7D), only one mode appears at 982 cm^{-1} in the Raman spectrum, which must be predominantly the $C_{14}D$ rock. The frequency shift from 986 to 982 cm^{-1}, plus the absence of any intensity for the $C_{15}D$ rocking modes indicate that the $C_{14}D$ and $C_{15}D$ rocks are somewhat coupled. The test developed by Fodor et al. relied on the near degeneracy of the $C_{14}D$ and $C_{15}D$ rocks which strongly split these modes into A- and B-symmetry combinations.[20] The C=N *syn* configuration in 12-*N*-ethano retinal has destroyed this near degeneracy of the rocks, and this molecule cannot, therefore, provide a test of the previous predictions.

A variety of modes with $C_{14}D$ and $C_{15}D$ rocking character appear in the calculation (Table I). A mode containing the largest 14D rock character is calculated at 888 cm^{-1} in the dideuterio compound that has similar normal mode description as that at 887 cm^{-1} in the 14D calculation. This is consistent with the relatively small shift that is observed in the 986-cm^{-1} 14D rock mode upon going to the 14,15-D$_2$ derivative. A B-symmetry combination between the 14D and 15D rocks is calculated at 1092 cm^{-1}. There is no corresponding mode of A symmetry. As discussed previously, neither of these modes is observed experimentally in either the Raman or the infrared spectra. Furthermore, the 15D rock mode at 900 cm^{-1} in the 15-D calculation shifts to 899 cm^{-1} in the dideuterio calculation with no significant change in character, and the 1040-cm^{-1} mode in the 15-D calculation shifts to 1041 cm^{-1} in the dideuterio calculation. These modes do change character somewhat, but the amount of $C_{15}D$ rock component does not change significantly. Thus, the MNDO calculation predicts that the modes involving the 14D and 15D rocks should be relatively insensitive to substitution at the other position, as observed.

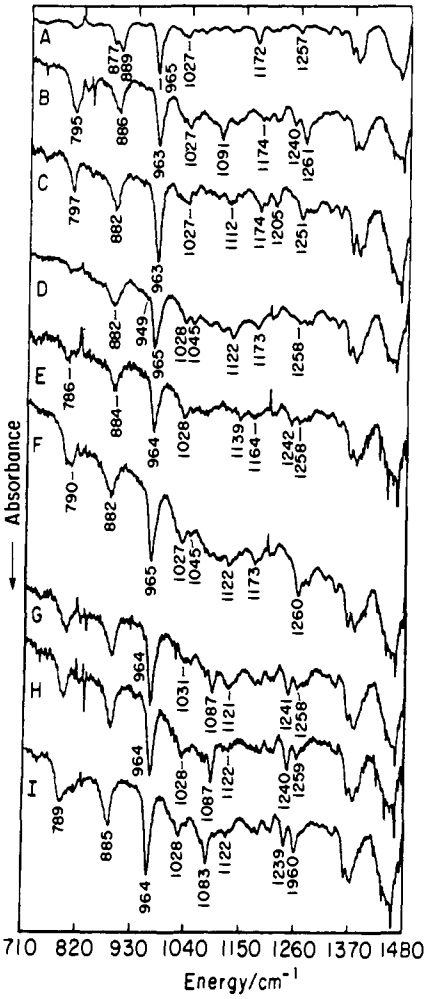

Figure 5. The infrared spectra of (A) 12-ethyl,13-cis Schiff base, (B) 12-*N*-ethano Schiff base and its (C) 14D, (D) 15D, (E) 14,15-^{13}C,15D, (F) 14,15D$_2$, (G) 14^{13}C, (H) 15^{13}C, and (I) 14,15-^{13}C derivatives. Infrared spectra were obtained from a thin film on a KBr window.

Conclusions

The goal of this work was to synthesize a retinal model compound having a known C_{14}–C_{15} conformation and study its vibrational properties. This is the first vibrational study on retinal model compounds having a defined geometry about the C_{14}–C_{15} and C=N bonds. Three key observations can be summarized.

(1) The C_{14}–C_{15} stretch in the locked 14-*s-cis* retinal has been assigned at 1096 cm^{-1} based on its infrared intensity and its sensitivity to ^{13}C substitution. This frequency supports earlier predictions that the C_{14}–C_{15} stretch in a 14-*s-cis* compound would lie ~70 cm^{-1} below that of a 14-*s-trans* Schiff base.[17] Thus, the frequency of the C_{14}–C_{15} stretch is indicative of the conformation about that bond in retinal Schiff bases.

(2) The $C_{15}D$ rock of a retinal chromophore having a C=N *syn* geometry has been studied for the first time. The $C_{15}D$ rock is shown to be coupled with the skeletal stretches to form mixed modes at ~1040 and 950 cm^{-1}. The appearance of a mode with $C_{15}D$ rock character at ~1040 cm^{-1} is characteristic of a C=N

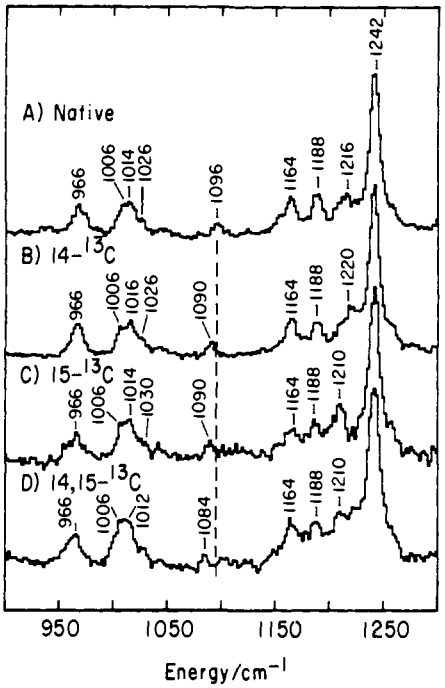

Figure 6. Raman spectra of (A) 12-*N*-ethano Schiff base and its (B) 14-^{13}C, (C) 15-^{13}C, and (D) 14,15-^{13}C derivatives.

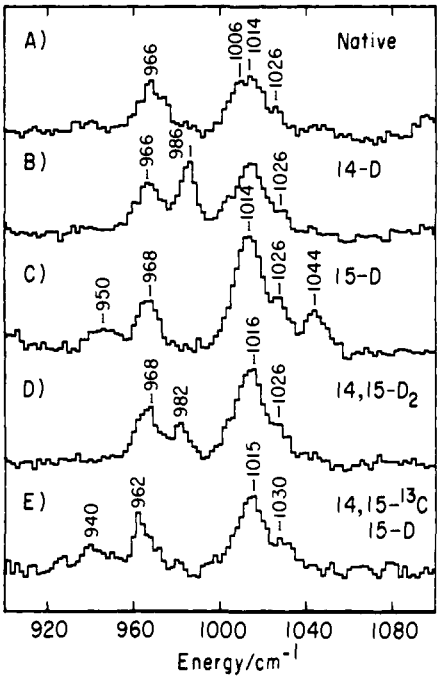

Figure 7. Raman spectra of the (A) 12-*N*-ethano Schiff base and its (B) 14D, (C) 15D, (D) 14,15D$_2$, and (E) 14,15-^{13}C,15D derivatives.

syn geometry. Previous work has shown that the appearance of a $C_{15}D$ rocking mode at ~970 cm^{-1} is characteristic of a C=N *anti* geometry. Thus, the work presented here demonstrates that the C=N configuration of retinal in pigments containing Schiff base chromophores may be reliably determined by using a $C_{15}D$ labeled compound, as has been argued earlier in the work of Ames et al.[27] This also provides an additional method for determining the C=N configuration of protonated Schiff bases since the $C_{15}D$ coupling pattern is not significantly altered by Schiff base protonation (see Ames et al., 1989).[27]

(3) Earlier studies suggested that the C_{14}–C_{15} conformation may also be determined based on the extent of coupling between the $C_{14}D$ and $C_{15}D$ rocks.[20] This test relies on the near degeneracy of the two deuteriated rocks. In our locked *s-cis* retinal, the $C_{15}D$ rock is no longer degenerate with the $C_{14}D$ rock due to the C=N *syn* configuration. Thus, this molecule cannot be used to provide a test of the earlier predictions.

Experimental Section

All experiments were carried out under a dry nitrogen atmosphere. THF was freshly distilled from $LiAlH_4$, petroleum ether (40–60 °C) and ether were distilled from P_2O_5 and stored over sodium wire, toluene was distilled from CaH_2 and stored over sodium wire, and methanol was distilled from Mg (5 g/L) and stored on 3-Å molecular sieves. Pyridine was distilled from CaH_2 and stored over 4-Å molecular sieves. The ^{1}H NMR spectra were recorded on a JEOL NM FX-200 or a Bruker WM-300 spectrometer. The ^{1}H noise-decoupled ^{13}C NMR spectra were recorded on a Jeol NM FX-200 at 50.1 MHz or on a Bruker MSL-400 spectrometer at 100 MHz ($CDCl_3$, 77 ppm). Mass spectra and label determinations were carried out using a Kratos MS 9/50 mass spectrometer. IR spectra were obtained using a Pye-Unicam SP 3-200 spectrophotometer, and UV–vis spectra were recorded with a Varian DMS 200 spectrophotometer. HPLC separations were performed using a Dupont 830, equipped with a Dupont spectrophotometer (detection at 360 nm) and a 25 cm × 22.5 mm Zorbax Sil column.

(1-^{13}C)Acetonitrile, (2-^{13}C)acetonitrile, and (1,2-$^{13}C_2$)acetonitrile (all with more than 90% ^{13}C incorporation) were obtained from Merck Sharp and Dohme Isotopes; all other reagents were obtained from Aldrich or Janssen Chimica.

2-(3-Methyl-5-(2,6,6-trimethyl-1-cyclohexenyl)-2,4-pentadienylidene)-γ-butyrolactone (3). A suspension of sodium hydride (411 mg, 10.2 mmol, 60% dispersion in oil) was washed with dry petroleum ether (3×) to remove the mineral oil. THF (50 mL) was added and the suspension was cooled to 0 °C. 2-(Diethylphosphono)-γ-butyrolactone (2.4 g, 11 mmol) dissolved in THF (10 mL) was added dropwise. After 15 min C_{15}-aldehyde **2** (1.60 g, 7.3 mmol), dissolved in THF (10 mL), was added, and stirring was continued for 30 min. Workup was accomplished by adding a saturated solution of ammonium chloride followed by extraction with ether (2×). The combined ether layers were washed with a saturated sodium chloride solution and dried ($MgSO_4$). Evaporation yielded a brown oil. Purification with column chromatography (elution with CH_2Cl_2) afforded **3** (2.02 g, 7.1 mmol, 96%) as yellowish crystals that could be recrystallized from ether/petroleum ether: mp 134 °C; IR (film in cyclohexane) 2920, 1735, 1630, 1200, 1025, 730 cm^{-1}; ^{1}H NMR δ 1.25 (s, 6 H, 1-$(CH_3)_2$), 1.50 (m, 2 H, H-2), 1.63 (m, 2 H, H-3), 1.73 (s, 3 H, 5-CH_3), 2.07 (s, 3 H, 9-CH_3), 3.00 (dt, J = 7.4, 2.7 Hz, 2 H, H-12a), 4.42 (t, J = 7.4 Hz, 2 H, H-12b), 6.00 (d, J = 12.3 Hz, 1 H, H-10), 6.21 (d, J = 16 Hz, 1 H, H-8), 6.45 (d, J = 16 Hz, 1 H, H-7), 7.53 (dt, J = 12.3, 2.7 Hz, 1 H, H-11); λ_{max} (EtOH) 345 nm. Exact mass 286.1930 (calcd for $C_{19}H_{26}O_2$: 286.1934).

3-(2-Acetoxyethyl)-6-methyl-8-(2,6,6-trimethyl-1-cyclohexenyl)-octa-3,5,7-trien-2-one (4). A solution of lactone **3** (1 g, 3.5 mmol, dried under vacuum) in THF (15 mL) was cooled slowly to −100 °C, and trimethylsilyl chloride (2.2 mL, 17.5 mmol), freshly distilled from CaH_2, was added. Under vigorous stirring, methyllithium (4.1 mL, 6.6 mmol) was added dropwise, keeping the temperature of the solution between −90 and −100 °C. After 15 min TLC analysis showed complete conversion of the starting compound to the product hydroxy ketone. Workup was accomplished by adding a slurry of silica gel (7 g) and water (2.8 g). Stirring was continued for 1 h at 0 °C, then water (10 mL) and ether (50 mL) were added, and the silica gel was removed by filtration. The organic layer was washed with water, followed by saturated sodium chloride solution (2×) and dried with $MgSO_4$. Evaporation of the solvent and purification of the residue with column chromatography (gradient: 20% to 50%, ether/petroleum ether) afforded the product hydroxy ketone (815 mg, 2.7 mmol, 77%) as a yellow oil.

The hydroxy ketone was dissolved in dry toluene (15 mL), 4-dimethylaminopyridine (423 mg, 3.5 mmol) and acetic anhydride (334 mg, 3.3 mmol) were added, and the mixture was stirred at room temperature for 2 h. Ether was added and after usual workup and evaporation of the solvents pure acetate (856 mg, 2.49 mmol; 92%) was obtained as a yellow oil: IR (film) 2920, 1730, 1650, 1590, 1265, 1235 cm^{-1}; ^{1}H NMR δ 1.04 (s, 6 H, 1-$(CH_3)_2$), 1.50 (m, 2 H, H-2), 1.63 (m, 2 H, H-3), 1.73 (s, 3 H, 5-CH_3), 1.98 (s, 3 H, 9-CH_3), 2.04 (bt, 2 H, H-4). 2.08 (s, 3 H, acetyl), 2.40 (s, 3 H, 13-CH_3), 2.80 (t, J = 6.8 Hz, 2 H, H-12a), 4.10 (t, J = 6.8 Hz, 2 H, H-12b), 6.23 (d, J = 16.0 Hz, 1 H, H-8), 6.40 (d, J = 11.9 Hz, 1 H, H-10), 6.45 (d, J = 16.1 Hz, 1 H, H-7), 7.57 (d, J = 11.9 Hz, 1 H, H-11). Exact mass: 345.2435 (calcd for $C_{22}H_{33}O_3$: 345.2431).

3,7-Dimethyl-4-(2-hydroxyethyl)-9-(2,6,6-trimethyl-1-cyclohexenyl)-nona-2,4,6,8-tetraenenitrile (5). A solution of anhydrous diisopropylamine (1.03 mL, 7.32 mmol) in THF (10 mL) was cooled to −20 °C, and *n*-butyllithium (4.6 mL, 1.6 M solution in hexane) was added. After stirring for 10 min, the solution was cooled to −80 °C and acetonitrile

(150 mg, 3.66 mmol) dissolved in THF (5 mL) was added dropwise. A white precipitate of lithioacetonitrile slowly formed. After stirring for 15 min at −80 °C, diethyl chlorophosphate (531 μL, 3.66 mmol) dissolved in THF (5 mL) was slowly added and the solution was allowed to warm to 0 °C over 1 h. Ketoacetate **4** (840 mg, 2.44 mmol) dissolved in THF (5 mL) was added to the clear yellowish solution. After stirring for 30 min at room temperature and subsequently 30 min at 45 °C, TLC (30% ether/petroleum ether) showed complete disappearance of the starting compound. Workup was accomplished by neutralizing the solution with a 10% HCl solution, extraction with ether (2×), and drying. After evaporation, crude acetoxy nitrile was obtained as a bright yellow oil. This crude product was dissolved in dry methanol (10 mL) and added dropwise to a 10% solution of KOH in methanol (50 mL) of −30 °C. During the addition the temperature of the solution did not exceed −20 °C. Stirring was continued for 1 h while the temperature was kept between −20 and −30 °C. Workup was accomplished by adding an ice-cold saturated solution of ammonium chloride (20 mL) and quickly neutralizing the mixture with concentrated HCl. Extraction with ether (2×), drying, and concentration afforded the crude hydroxy nitrile **5** as a dark yellow oil. Purification with column chromatography (30% to 50% ether in petroleum ether) gave **5** (619 mg, 1.90 mmol; 78% based on **4**) as a yellow oil: IR (film) 3430, 2900, 2200, 1560, 1040, 900, 860 cm^{-1}; ^1H NMR δ 1.04 (s, 6 H, 1-$(CH_3)_2$), 1.47 (m, 2 H, H2), 1.60 (m, 2 H, H-3), 2.03 (s, 3 H, 9-CH_3), 2.31 (s, 3 H, 13-CH_3), 2.73 (t, J = 7.1 Hz, 2 H, H-12a), 3.68 (bt, 2 H, H-12b), 5.43 (s, 1 H, H-14), 6.21 (d, J = 16.1 Hz, 1 H, H-8), 6.37 (d, J = 16.1 Hz, 1 H, H-7), 6.37 (d, J = 12.0 Hz, 1 H, H-10), 7.02 (d, J = 12.0 Hz, 1 H, H-11).

(14-^{13}C)5 (5a). (2-^{13}C)Acetonitrile (150 mg, 3.57 mmol) was treated as described for **5** to afford ^{13}C-labeled nitrile **5a** (548 mg, 1.86 mmol, 71%): ^1H NMR identical with **5** except for the resonance at δ 2.31 (d, $^3J_{CH}$ = 6.2 Hz, 3 H, 13-CH_3) and δ 5.43 (d, $^1J_{CH}$ = 70.3 Hz, 1 H, H-14); ^{13}C NMR δ 93.9.

(15-^{13}C)5 (5b). Similarly, (1-^{13}C)acetonitrile (150 mg, 3.57 mmol) was treated as described for **5** to afford ^{13}C-labeled nitrile **5b** (598 mg, 1.83 mmol; 77%): ^1H NMR identical with **5** except for a slight broadening of the resonance at δ 5.43; ^{13}C NMR δ 118.

(14,15-$^{13}C_2$)5 (5c). The same procedure as described for **5** was used to convert (1,2-$^{13}C_2$) acetonitrile (150 mg, 3.49 mmol) into $^{13}C_2$-labeled nitrile **5c** (560 mg, 1.70 mmol; 72%); ^1H NMR identical with **5a**; ^{13}C NMR: δ 118.6 (d, $^1J_{CC}$ = 80.6 Hz), 93.9 (d, $^1J_{CC}$ = 80.6 Hz).

(14-^{2}H)5 (5d). C^2H_3CN (150 mg, 3.44 mmol) was used to convert **4** into **5d**. Workup of the HWE reaction was accomplished by acidifying the mixture with $^2HCl/^2H_2O$ to pH 3. After the solution was stirred for 5 min, ether was added and the mixture was neutralized with $NaHCO_3$ solution. The remainder of the procedure was identical with the preparation of **5** to furnish **5d** (560 mg, 1.90 mmol, 73%): ^1H NMR identical with **5**, except for the loss of 85% of the original intensity at δ 5.43.

3,7-Dimethyl-4-(2-azidoethyl)-9-(2,6,6-trimethyl-1-cyclohexenyl)-nona-2,4,6,8-tetraenenitrile (6). A solution of 440 mg (1.35 mmol) of hydroxy nitrile **5** in dry pyridine (20 mL) was cooled to 0 °C. Then *p*-toluenesulfonyl chloride (515 mg, 2.70 mmol) was added; stirring was continued at 0 °C. After 6 h, another equivalent of tosyl chloride was added (260 mg) and the solution was stored overnight at −15 °C. Workup was accomplished by adding a 1 N solution of HCl (50 mL) and extracting the mixture with ether (3×). Drying and concentration afforded a dark-brown oil that was purified with column chromatography (20% ether/petroleum ether) to afford the intermediate tosyl nitrile (471 mg, 0.97 mmol, 72%) as a bright yellow oil.

The tosyl nitrile (471 mg, 0.97 mmol) was dissolved in dimethylformamide (20 mL) containing 3 drops of water. Sodium azide (126 mg, 1.94 mmol) was added and the mixture was stirred at 100 °C for 1 h. Workup was accomplished by adding ether (50 mL) and washing the mixture with water (10 mL × 5). Drying and concentration afforded the nearly pure azido nitrile. Purification with a short column (eluent 30% ether/petroleum ether) gave pure **6** (312 mg, 0.89 mmol, 92%) as a dark yellow oil: IR (film) 2900, 2200, 2090, 1600, 1560, 960, 850 cm^{-1}. Exact mass: 350.2474 (calcd for $C_{22}H_{30}N_4$: 350.2473).

^1H NMR: δ 1.04 (s, 6 H, 1-$(CH_3)_2$), 1.47 (m, 2 H, H-2), 1.62 (m, 2 H, H-3), 1.74 (s, 3 H, 5-CH_3), 2.04 (s, 3 H, 9-CH_3), 2.31 (s, 3 H, 13-CH_3), 2.71 (t, J = 7.4 Hz, 2 H, H-12a), 3.32 (t, J = 7.4 Hz, 2 H, H-12b), 5.35 (s, 1 H, 14-H), 6.22 (d, J = 16.0 Hz, 1 H, H-8), 6.30 (d, J = 12.0 Hz, 1 H, H-10), 6.39 (d, J = 16.0 Hz, 1 H, H-7), 7.00 (d, J = 12.0 Hz, 1 H, H-11).

(14-^{13}C)6 (6a). Following the procedure as described for **6**, **5a** was converted into the corresponding tosylate (0.97 mmol, 60%); reaction with NaN_3 yielded **6a** (300 mg, 0.85 mmol, 88%): ^1H NMR identical with **6** except for doublets at δ 5.35 ($^1J_{CH}$ = 69.8 Hz) and at δ 2.31 ($^3J_{CH}$ = 6.1 Hz); ^{13}C NMR δ 93.8.

(15-^{13}C)6 (6b). Similarly, 1.83 mmol of **5a** gave 0.96 mmol (53%) of the corresponding tosylate which was subsequently converted into **6b** (332 mg, 0.95 mmol, 99%): ^1H NMR identical with **6**; ^{13}C NMR δ 118.4.

(14,15-$^{13}C_2$)6 (6c). From **5c**, the corresponding tosylate was obtained (0.98 mmol, 59%), which was then converted into **6c** (330 mg, 0.94 mmol, 96%): ^1H NMR identical with **6a**; ^{13}C NMR doublets at δ 118.4 ($^1J_{CC}$ = 82.1 Hz) and δ 93.8 ($^1J_{CC}$ = 82.1 Hz).

(14-^{2}H)6 (6d). **6d** (315 mg, 0.90 mmol) was similarly prepared via the tosylate (55%) in 86% yield: ^1H NMR identical with **6** except for the loss of 85% of the original intensity at δ 5.35.

12-*N*-Ethanoretinylimine (1). Azido nitrile **6** (100 mg, 0.29 mmol) was dissolved in petroleum ether (10 mL). The solution was cooled to −60 °C and diisobutylaluminium hydride (0.9 mL, 1 M solution in hexane) was added. Stirring was continued for 1 h, during which time the mixture was allowed to warm to room temperature. TLC analysis in ether/petroleum ether/methanol (5/5/1 v/v) showed a yellow- and a red-colored product with R_f values of 0.50 and 0.45, respectively. The mixture was cooled to 0 °C and, while stirring vigorously, methanol (0.25 mL) was added followed by acetic acid (10 M, 0.1 mL). The solution turned bright-red (the pH was kept between 5.5 and 6.5). After stirring at 0 °C for 30 min, 3-Å molecular sieves were added and stirring was continued for 15 min. The mixture was filtered over Celite and rinsed thoroughly with small portions of dry methanol. The mixture was made slightly alkaline with a 10% NaOH solution (the red solution turns yellow) and then extracted with ether. Drying and concentration afforded a mixture of seven-membered ring amine **1** and five-membred ring imine **7**. Purification with column chromatography (eluent: ether/petroleum ether/methanol 5:5:1 and a few drops of triethylamine) afforded the pure seven-membered ring imine **1** (28 mg, 0.09 mmol, 32%) as a mixture of two isomers (9*E* and 9*Z*). The 7*E*,9*E*,11*E* isomer was obtained in pure form by HPLC (eluent: ether/petroleum ether/methanol 5:5:1 v/v at a flow rate of 20 mL/min; detection at 360 nm; retention time of 9.5 min): IR (film) 2900, 1440, 970 cm^{-1}; ^1H NMR δ 1.03 (s, 6 H, 1-$(CH_3)_2$), 1.49 (m, 2 H, 2-H), 1.60 (m, 2 H, 3-H), 1.73 (s, 3 H, 5-CH_3), 2.00 (s, 3 H, 9-CH_3), 2.05 (bt, 2 H, 4-H), 2.14 (s, 3 H, 13-CH_3), 2.71 (m, 2 H, H-12a), 3.87 (m, 2 H, 12b), 5.80 (d, J = 4.5 Hz, 1 H, 14-H), 6.19 (d, J = 16.1 Hz, 1 H, 8-H), 6.29 (d, J = 16.1 Hz, 1 H, 7-H), 6.35 (d, J = 12.2 Hz, 1 H, 10-H), 6.64 (d, J = 12.2 Hz, 1 H, 11-H), 7.75 (d, J = 4.5 Hz, 1 H, 15-H); ^{13}C NMR δ 12.79 (C-19), 19.20 (C-3), 21.77 (C-18), 23.33 (C-20), 28.95 (C-16/17), 33.09 (C-4), 34.25 (C-1), 39.57 (C-2), 51.90 (C-12a), 59.35 (C-12b), 121.96 (C-14), 125.15 (C-11), 125.24 (C-10), 128.41 (C-7), 130.02 (C-5), 137.68 (C-6), 137.76 (C-8), 139.08 (C-12), 139.65 (C-9), 147.63 (C-13), 159.38 (C-15); UV–vis (EtOH) λ_{max} 378.3 nm. Exact mass: 309.2462 (calcd for $C_{22}H_{31}N$: 309.2458).

Similarly, 100 mg of (14-^{13}C)**6a**, (15-^{13}C)**6b**, (14,15-$^{13}C_2$)**6c**, and (14-^{2}H)**6d** have been converted into respectively (14-^{13}C)**1a**, (15-^{13}C)**1b**, (14,15-$^{13}C_2$)**1c**, and (14-^{2}H)**1d**. The overall yield based on the labeled acetonitriles is 16%. Reduction of azido nitrile **6**, (14-^{2}H)**6d**, and (14,15-$^{13}C_2$)**6c** with 3 equiv of Dibal-^2H, according to the procedure described above, afforded respectively (15-^{2}H)**1e**, (14,15-$^2H_2$)**1f**, and (14,15-$^{13}C_2$,15-^{2}H)**1g**.

Double-focus mass spectrometry of the labeled compounds **1a–g** gives the following m/z values for the parent peak and isotope incorporations.

1a: 310.2487 (calcd for $^{12}C_{21}{}^{13}C_1H_{31}N$: 310.2492), 93% ^{13}C incorporation.

1b: 310.2500 (calcd for $^{12}C_{21}{}^{13}C_1H_{31}N$: 310.2492), 90% ^{13}C incorporation.

1c: 311.2530 (calcd for $^{12}C_{20}{}^{13}C_2H_{31}N$: 311.2525), 82% di-^{13}C and 18% mono-^{13}C incorporation.

1d: 310.2521 (calcd for $^{12}C_{22}{}^1H_{30}{}^2H_1N$: 310.2519), 85% ^{2}H incorporation.

1e: 310.2522 (calcd for $^{12}C_{22}{}^1H_{30}{}^2H_1N$: 310.2519), 98% ^{2}H incorporation.

1f: 311.2583 (calcd for $^{12}C_{22}{}^1H_{29}{}^2H_2N$: 311.2580); 83% di-^{2}H and 16% mono-^{2}H incorporation.

1g: 312.2587 (calcd for $^{12}C_{20}{}^{13}C_2{}^1H_{30}{}^2H_1N$: 312.2586), 82% di-^{13}C, 98% mono-^{2}H.

In the 300-MHz ^1H NMR spectra of the ^{13}C- and ^{2}H-labeled compounds, the chemical shifts and the ^1H–^1H coupling constants are identical with those found for **1**. In the spectra of (14-^{13}C)**1a**, (15-^{13}C)**1b**, (14,15-$^{13}C_2$)**1c**, and (14,15-$^{13}C_2$,15-^{2}H)**1g**, in addition, $^1J_{CH}$, $^2J_{CH}$, and $^3J_{CH}$ coupling constants are observed, which establish the presence of the ^{13}C label at the expected position. These values are summarized in Table II. In the 300-MHz ^1H NMR spectra of (14-^{2}H)**1d**, (15-^{2}H)**1e**, (14,15-$^2H_2$)**1f**, and (14,15-$^{13}C_2$,15-^{2}H)**1g**, the disappearance of the expected signal(s) clearly shows the position of the ^{2}H isotope. Accurate integration confirms the amount of enrichment found by mass spectrometry.

In the ^1H noise-decoupled 100-MHz ^{13}C NMR spectra of the mono-^{13}C-enriched compounds **1a** and **1b**, one strong peak due to the ^{13}C

Table II. $^{13}C-^{1}H$ and $^{13}C-^{13}C$ Coupling Constants (Hz) in **1**

$^{1}J(^{13}C-^{1}H)$		$^{1}J(^{13}C-^{13}C)$	
$C_{14}-H_{14}$	153.0	$C_{14}-C_{15}$	48.8
$C_{15}-H_{15}$	173.3	$C_{14}-C_{13}$	61.8
$^{2}J(^{13}C-^{1}H)$		$^{3}J(^{13}C-^{13}C)$	
$C_{14}-H_{15}$	10.6	$C_{14}-C_{12a}$	4.5
$C_{15}-H_{14}$	<1.5	$C_{14}-C_{11}$	6.0
		$C_{15}-C_{12a}$	broadening
$^{3}J(^{13}C-^{1}H)$		$C_{15}-C_{12}$	5.1
$C_{14}-C_{13}H_3$	7.5	$C_{15}-C_{13}H_3$	broadening

enrichment is found at the expected chemical shift value, at 122.0 and 159.3, respectively. In the spectrum of the $^{13}C_2$-enriched compound **1c**, at 122.0 and 159.3 an AB pattern [$^{1}J(^{13}C-^{13}C)$ = 48.8 Hz] is observed, together with the singlets due to the 2× 10% monolabeled material, which is in agreement with the enrichment determined by mass spectrometry. The spectra clearly demonstrate that no scrambling has occurred. The ^{13}C-enriched compounds also contain the natural abundance amount (1.1%) of ^{13}C at each of the nonenriched positions. This implies that in the singly labeled compounds ^{13}C pairs involving the enriched position are present at a level of approximately 1% (0.9 × 1.1%). From the ^{1}H noise-decoupled 100-MHz ^{13}C NMR spectra at the natural abundance level, the $^{13}C-^{13}C$ coupling constants are obtained. The values are summarized in Table II. In the proton noise-decoupled 50-MHz ^{13}C NMR spectra of the deuteriated seven-membered rings **1d**, **1e**, and **1f**, the deuterium-carrying carbon atom has a low intensity or is lost in the noise owing to the low magnetic moment and the absence of the NOE.[39]

(39) Breitmeier, E.; Voelter, W. *Carbon-13 NMR Spectroscopy*, 3rd ed.; VCH Gesellschaft: Weinheim, 1987.

Direct Observation of Intramolecular Hydrogen Bonding of a Hydroxy Proton to an Indenide Carbanion in Apolar and Polar Non-Hydrogen Bond Donor Solvents by NMR and IR Spectroscopy

Ian Mc Ewen and Per Ahlberg*

Contribution from the Department of Organic Chemistry, University of Göteborg, S-412 96 Göteborg, Sweden. *Received June 22, 1992*

Abstract: To obtain information about the elusive hydrogen-bonded carbanions, which are postulated as intermediates in proton-transfer reactions from carbon acids, the molecule 4-(3′-indenyl)-2,3,4-trimethyl-2-pentanol (**1**) has been designed and synthesized. The carbanion **2** generated in polar non-hydrogen bond donor solvents from the precursor **1** showed the presence of long-lived intramolecular hydrogen bonding of the hydroxy group to the carbanionic part (cf. **2a**). It was discovered that in the presence of cryptand C211 carbanion **2** rather than the oxyanion **3** was formed in apolar non-hydrogen bond donor solvents upon reaction of **1** with butyllithium. An extensive study of this interaction in solvents like dimethyl sulfoxide (DMSO), tetrahydrofuran (THF), pyridine, benzene, and toluene using NMR and IR spectroscopy has been carried out. For example, in benzene the OH proton in **2** appeared in the ^{1}H NMR spectrum 3.2 ppm downfield of the corresponding proton in the precursor **1**. In the IR spectrum, the OH stretching band of **2** appeared shifted 274 cm^{-1} to lower frequency relative to that of **1**. Also consistent with the structure **2a** for carbanion **2** was the observed small temperature dependence of the ^{1}H NMR chemical shift of the OH proton which is typical for intramolecular hydrogen bonding. Nuclear Overhauser enhancement (NOE) studies also strongly support the proposed structure **2a** for the carbanion.

Introduction

Knowledge about the elusive hydrogen-bonded carbanions, which are postulated as intermediates in proton-transfer reactions, is meager, as is the knowledge of the specific solvation of carbanions in general. There are only a few reports on hydrogen bonding by bulk solvent to carbanions[1] and hydrogen bonding to an isonitrile.[2] In the solid state, crystallographic studies have shown the presence of hydrogen bonding to carbanions,[3] and in the gas phase the strength of hydrogen bonds to acetylides has been measured using ion cyclotron spectroscopy.[4]

Our work in this area has been focused on designing reaction systems with the potential to yield hydrogen-bonded carbanions

Scheme I

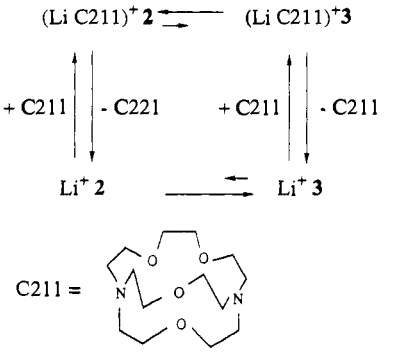

with lives long enough to allow direct observation of such species by NMR, IR, and UV spectroscopy.[5]

In our attempts to develop systems with hydrogen bonding of OH to the carbanions, we initially used DMSO[6] as solvent and

(1) (a) Ford, W. T. *J. Am. Chem. Soc.* **1970**, *92*, 2857. (b) Hogen-Esch, T. E. *J. Am. Chem. Soc.* **1973**, *95*, 639. (c) Greifenstein, L. G.; Pagani, G. A. *J. Org. Chem.* **1981**, *46*, 3336. (d) Mueller-Westerhoff, U. T.; Nazzal, A.; Proessdorf, W. *J. Am. Chem. Soc.* **1981**, *103*, 7678.

(2) (a) Ferstandig, L. L. *J. Am. Chem. Soc.* **1962**, *84*, 1323. (b) Ferstandig, L. L. *J. Am. Chem. Soc.* **1962**, *84*, 3553. (c) Schleyer, P. v. R.; Allerhand, A. *J. Am. Chem. Soc.* **1962**, *84*, 1322. (d) Allerhand, A.; Schleyer, P. v. R. *J. Am. Chem. Soc.* **1963**, *85*, 866.

(3) (a) Seebach, D. *Angew. Chem.*, Int. Ed. Engl. **1988**, *27*, 1624. (b) Buchholz, S.; Harms, K.; Massa, W.; Boche, G. *Angew. Chem.* **1989**, *101*, 73.

(4) Caldwell, G.; Rozeboom, M. D.; Kiplinger, J. P.; Bartmess, J. E. *J. Am. Chem. Soc.* **1984**, *106*, 4660.

(5) (a) Ahlberg, P.; Johnsson, B.; Mc Ewen, I.; Rönnqvist, M. *J. Chem. Soc., Chem. Commun.* **1986**, 1500. (b) Ahlberg, P.; Davidsson, Ö. *J. Chem. Soc., Chem. Commun.* **1987**, 623. (c) Ahlberg, P.; Davidsson, Ö; Johnsson, B.; Mc Ewen, I.; Rönnqvist, M. *Bull. Soc. Chim. Fr.* **1988**, *2*, 177. (d) Mc Ewen, I.; Ahlberg, P. *J. Chem. Soc., Chem. Commun.* **1989**, 1198.

0002-7863/92/1514-10869$03.00/0 © 1992 American Chemical Society